Grain boundaries and impurities in CdTe/CdS solar cells

K. Durose[a,*], M.A. Cousins[a], D.S. Boyle[a,1], J. Beier[b], D. Bonnet[b]

[a]*Department of Physics, University of Durham, South Road, Durham DH1 3LE, UK*
[b]*ANTEC GmbH, 2–4 Industriestrasse, Kelkheim/Ts, Germany*

Abstract

Near-interface grain effects and quantitative SIMS impurity profiles for close-space sublimation-deposited CdTe/CdS solar cells and test structures are described. TEM of the interfacial CdTe grains demonstrated them to be smaller than expected from extrapolation of the bulk grain size. Computer simulation showed this to be consistent with the development of grain sizes during additive growth processes, the grain size increasing approximately as the root distance from the polycrystalline hetero-interface. TEM of the near-interfacial CdTe before and after $CdCl_2$ processing revealed grain growth from 0.1 to 0.5 μm — even though the grain size distribution in the overlying CdTe is stable to processing. Quantitative SIMS of test structures comprising co-sputtered contacts on close-space sublimation-deposited cells (Sb–Te/CdTe/CdS/TCO/glass) is reported for the structures in their fresh, light-soaked and bake-tested states. High concentrations of impurities are present in the CdTe of the fresh cells as follows: S, 7×10^{19}; Cl, 8×10^{18}; Cu, 7×10^{17}; Na, 3×10^{17}; Sb, 4×10^{18}; and O, 7×10^{18} cm^{-3}. It is considered that the unintentionally introduced impurities are unlikely to originate from the source CdTe. The effects upon the impurity distributions of light soaking and baking in air at 400°C are reported. Accumulations of impurities near to the CdS layer are discussed. © 2002 Elsevier Science B.V. All rights reserved.

Keywords: CdTe/CdS; Grain boundaries; Recrystallisation; Impurities; Secondary-ion mass spectrometry (SIMS)

1. Introduction

The design, processing, performance and materials aspects of CdTe/CdS solar cells are reviewed extensively elsewhere. For a general review, the reader is referred to that of Birkmire and Eser [1], and for materials topics to Durose et al. [2]. The object of the present work is to present new results on (a) grain size distributions and (b) quantitative impurity determinations in close-spaced sublimation (CSS)-grown CdTe/CdS solar cells.

In polycrystalline solar cells, grain boundaries are considered important, since they potentially influence: (a) carrier recombination; (b) carrier transport — by the influence of the grain boundary potentials; and (c) diffusion processes in the cell material. An enduring and general model of the electrical structure of grain boundaries is that due to Werner et al. [3], in which states above the Fermi level are charged and a local field results. The resultant electrical barrier has a height dependent upon the sheet charge density at the grain boundary. Using Werner's method of sub-bandgap photoconductance spectroscopy of grain boundaries, the grain boundary density of states in silicon is found to be in the range 10^{14}–10^{17} m^2 eV [4], this being similar to that in CdTe bicrystals [5]; grain boundaries might be considered deleterious for both kinds of cell. However, the grain boundary density of states is a function of the impurities in CdTe (at least), and the only measurements reported for CdTe [5] were for material containing dopants, which are very different from modern $CdCl_2$-treated devices. Indeed, recent models of the electrical environment of grain boundaries in p-Cd/Te (in devices) invoke local upward band-bending that would act to repel minority carrier electrons. The models due to Woods et al. [6] and Galloway et al. [7] share

---

* Corresponding author. Tel.: +44-191-374-2395; fax: +44-374-7358.

E-mail address: ken.durose@durham.ac.uk (K. Durose).

[1] Present address: Department of Chemistry, University of Manchester, Oxford Road, Manchester M13 9PL, UK.

this feature, but differ in detail, with the former allowing for electron capture close to the boundary interface.

The literature on processing of CdTe/CdS solar cells contains widespread reports of grain growth phenomena, particularly under the influence of the ubiquitous $CdCl_2$ processing. Some general trends have emerged. Microstructural changes reported fall into the classical scheme of the development of defective polycrystalline materials, i.e. recovery, recrystallisation and grain growth. These changes are mediated by high temperatures, long annealing times and the presence of fluxing agents (in this case $CdCl_2$). Moutinho and co-workers' papers examine the dynamics of such processes and, importantly, demonstrate that *grain size* rather than preparative method is the factor that predisposes CdTe films to grain growth [8]. Material having grains <1 μm in size (e.g. electrochemically or magnetron sputter deposited) undergoes more grain growth than larger grained material (e.g. CSS films grown at high temperature). Indeed, CSS-grown CdTe films are widely reported not to undergo grain growth at all, although most such reports are for surface studies. The bevel profiling work of Cousins and Durose [9] also demonstrates that the as-grown distribution of grain sizes within the bulk of CSS-grown CdTe layers is stable to annealing with $CdCl_2$ at 400°C. However, Cousins' optical/etching method did not probe near-interface grains. Loginov et al. [10] reported limited cross-section TEM indicating grain growth at the near-interface region, but this was for cells grown under conditions that differed from those of Cousins. Hence, there is some uncertainty as to whether this interface grain structure is stable to processing or not in CSS-grown cell material for which there is an apparently stable bulk grain structure.

Much is known about the electrical activity of specific impurities and native defects in single-crystal CdTe (see review [11]). However, for polycrystalline CdTe solar cells, the materials used are impure by semiconductor standards (e.g. 99.999%). Moreover, the p-doping is *not* achieved by the conventional means, i.e. by introducing a controlled concentration of an acceptor with known identity. Instead, the as-grown materials are annealed in the presence of $CdCl_2$, whereupon the CdTe becomes 'activated' or 'type converted' from n- to p-type. The influence of this process on the performance, electro-optic and microstructural properties of CdTe/CdS solar cells are all widely reported, but the doping mechanism are not identified. It is speculated that the A-centre $[V_{Cd}-Cl_{Te}]$ is important. Also, oxygen when introduced during $CdCl_2$ processing is thought to slightly enhance cell performance. There are also several reports (see [12,13], for example) of Cl accumulating in the CdS layer.

Native defects are expected to play an important role. Indeed, there is considerable empirical evidence that Te-rich CdTe is necessary for good solar performance. For example, Chou and Rohatgi [14] demonstrated that Te-rich metal–organic vapour-phase epitaxy (MOVPE)-grown CdTe produces cells with higher efficiency than Cd-rich material. Furthermore, it is widely known that etching to give a Te-rich surface is essential for producing conducting electrical contacts to CdTe. Levi et al. [15] demonstrated that this procedure causes Te enrichment of the grain boundaries in the CdTe deep within the absorber layer. This may be associated with grain boundary passivation, as shown by EBIC [16].

Of the other potentially electrically active centres in the solar cell structure, Cu is the most widely studied owing to its use in contacting [12]. Many US teams use Cu doping to form a p^+ layer for contacting to CdTe. There has been some controversy about this and some EU workers prefer to use Sb_2Te_3, a narrow-gap p-contact material. Indeed, Asher et al. [17] reported that high levels of Cu can cause degradation. Cu appears to accumulate in the CdS, and Dobson et al. [12] consider that it diffuses from the contact surface, perhaps in association with Cl. Na is thought to out-diffuse from the glass substrate, but the evidence that it is beneficial to cell performance is very circumstantial indeed [18].

Overall, impurities and doping in CdTe/CdS solar cells are under-investigated. It is not known how the p-n junction is doped: There are however, empirical recipes for making good junctions.

2. Experimental

2.1. Grain boundary study

Solar cells with the structure CdTe/CdS/TCO/glass were prepared by CSS as described by Cousins and Durose [9] (TCO is transparent conducting oxide–indium tin oxide, with an over-layer of tin oxide in this case). The CSS deposition temperature was 500°C, while $CdCl_2$ treatment was carried out for 20 min at 400°C. This and an as-grown control sample were examined by TEM. Thin sections of the near-interface CdTe were prepared for TEM study in the plan-view geometry in the following way. First, the glass was removed by a combination of grinding and dissolution in HF (the TCO acts as an etch stop layer). Secondly, the sample was thinned to optical transparency by iodine ion-beam thinning from the contact side of the CdTe. At this point, the CdTe is guaranteed to be <1 μm thick. Finally, the samples were ion beam-thinned from the front surface to remove the TCO and CdS. TEM was carried out in a JEOL 200CX instrument. The grain size distribution was analysed from diffraction contrast images using the computer procedure described in [9] (for optical micrographs), with 30–100 grains being examined for each sample studied.

A computer model was developed to simulate the form of the evolution of grain size during growth of the

CdTe layer on a polycrystalline CdS substrate. The simulation took place in a cube made up of cells of dimensions $100 \times 100 \times 100$ units. A polycrystalline field representing the CdS was created in the $z = 0$ plane by generating a predetermined number of nuclei and growing them to fill the plane completely. In this way, the 100×100 network was divided into sub-fields representing grains of average area G_A. Growth proceeded by the arrival of new species of unit cube dimension. These joined the surface at random positions and were able to migrate, stop and then become associated with a particular grain. These decisions were reached with the aid of a normalised bonding parameter:

$$\sigma_n = \sum_{i=1}^{i=n} r_i^{-2} \Big/ \sum_{j=1}^{j=26} r_j^{-2} \qquad (1)$$

This can be defined for each position on the surface and is simply the sum of $1/r^2$ terms for all of the first, second and third nearest neighbours (i) of a particular position. The normalisation term is the maximum value of this sum, i.e. the sum of $1/r^2$ terms for all the 26 nearest neighbours (j) of a cube in the bulk structure. Varying degrees of surface mobility were incorporated in the model as follows: a bonding (attraction) term was defined as $P_A = P_S \times \sigma_n$ and compared to a random number R ($0 < R < 1$), where P_S is a scaling term that is constant for a given simulation. Only if $P_A > R$ — that is the species is at a strongly bonded site — does migration stop. Otherwise, migration is via nearest neighbour translations in random directions. Hence, the magnitude of P_S determines the degree of surface mobility, with small values of P_S favouring high mobility. Designation of the grain to which a stationary species belongs is as follows. If the occupied members of the set of 26 nearest neighbours are wholly contained in one grain, then the species belongs to that grain. Should the species straddle two grains, then the grain designation is decided by comparing the strength of bonding to the nearest neighbour in each of the two grains. To do this, bonding terms like σ_n are written for each grain and the species is designated as belonging to the grain to which it is most strongly bonded, i.e. the one with highest σ_n. Simulations were run for average substrate grain areas (G_A) in the range 1–64, and for mobility terms P_S in the range 10^{-2}–1. (It should be noted that the cubic species used in this growth model cannot be correlated directly with atoms or unit cells, rather the model is designed to test whether grain size development can arise from additive crystal growth processes.)

2.2. SIMS investigation of impurities in Sb-Te/CdTe/CdS/TCO/glass test structures

Test structures similar to full cell structures were fabricated for SIMS analysis. The basic material was

prepared as follows. CdS and CdTe were deposited on TCO-coated glass by CSS at 500°C by ANTEC GmbH. This was treated in CdCl$_2$ vapour in the usual way. In order to eliminate errors in SIMS profiling due to surface roughness, the CdTe surfaces were then polished by chemo-mechanical means in bromine/methanol/ethylene glycol. A contact structure of Sb–Te (~ 100 nm) was then co-sputtered at room temperature. To avoid roughening, the surface was not pre-conditioned by any etching before the contact was applied.

For SIMS analysis, these samples were then subjected to one of three procedures:

1. No further treatment, 'fresh cell';
2. 'Light soaked' for 1 week at 85°C under ~ 1-sun illumination, open circuit; and
3. Subjected to a diffusion/oxidation test by baking in air at 400°C for 30 min, i.e. 'bake tested'.

Quantitative dynamic SIMS profiling was conducted by MATS UK Ltd. using the Cs–metal cluster (CsM$^+$) method. Ion-implanted reference samples of S, O, Cl, Na, Cu and Sb were prepared on oriented CdTe Te($\bar{1}\bar{1}\bar{1}$)B surfaces by ion implantation, and these were used to determine the sensitivity factors in SIMS.

3. Results and discussion

3.1. Grain growth, grain size development and device efficiency

Plan-view TEM micrographs of the near-interface CdTe from the as-deposited and CdCl$_2$-treated solar cells is compared in Fig. 1a,b. The frequency histograms for grain sizes taken from these micrographs and the adjacent fields of view compared well with Rayleigh distributions — as was previously found for grains in the bulk of the layer [9]. The average grain-size values extracted from the data were 0.1 μm for the as-deposited and 0.5 μm for the CdCl$_2$-treated sample. These data points are compared with the data obtained from the grain size distributions in the bulk of the layers in Fig. 2. It is notable that the near-interface grain sizes do not appear to fit the trend for the bulk of the layer: the data for the bulk of the film appear to fit a straight line that shows no sign of a downward trend near to the interface. This apparent discontinuity might be rationalised as follows. Firstly, the bulk data were from optical micrographs. As optical microscopy is unable to resolve small grains, the average grain size for populations containing small grains will be over-estimated. Secondly, since the grain size of the underlying CdS layer is small (50 nm), it is expected that the locally epitaxial CdTe grains near to the interface have a correspondingly small size. Hence, the small interfacial grains are to be expected and the results from the bulk and the interface are likely to be self-consistent.

Fig. 1. Plan-view transmission electron micrographs of the near-interface CdTe in: (a) as-deposited solar cell material and (b) the cell after processing with $CdCl_2$. Statistical analysis of these and adjacent areas indicated an increase in grain size from 0.1 to 0.5 μm.

From the TEM results, it is therefore shown that for these CSS-grown cells, $CdCl_2$ processing effects near-interface grain growth in layers for which the bulk grain distribution is otherwise stable to processing. This resolves an apparent contradiction in the literature [9,10]. This finding is also consistent with the classical principle that grain growth effects are accelerated in small-grained samples.

The feasibility of the hypothesis that grain growth *alone* could result in the increase in J_{sc} observed upon $CdCl_2$ treatment was explored by a simple calculation. For these as-deposited and $CdCl_2$-treated cells, the AM1.5 J_{sc} values are 12.6 and 21.5 mA cm^{-2}, respectively (for more detail see [9]), i.e. J_{sc} is almost doubled for a five-fold increase in grain size. The calculation made the assumption that photo-excited carriers sweep through the cells with uniform areal density. Those that pass within a capture distance t of a grain boundary interface recombine and are lost. The aim was to calculate the capture distance, and this was carried out by assuming that grain boundary capture was the only

loss mechanism — and that the grain boundaries are electrically similar, both before and after processing. Using a lattice of hexagonal columnar grains, the capture length t satisfying both the grain size and J_{sc} data for both cells was found to be 32 nm. This implies that minority carriers coming within 32 nm of a grain boundary are captured and recombine. This type of model is consistent with the double-barrier model of Woods et al. [6]. But although the principle of grain boundary loss is shown here to be mathematically possible, the assumptions made are unphysical. It is very likely that other loss mechanisms operate and that they differ before and after processing. Similarly, current transport and EBIC measurements indicate that the grain boundaries undergo profound electrical change upon processing. It might be concluded that grain size itself is only one of a number of factors that influence this type of cell.

The computer model of growth further explores whether the phenomenon of small interfacial grains is consistent with a physical growth mechanism. The results of grain growth simulations in a $100 \times 100 \times 100$ cell volume are shown in Fig. 3. Simulations for growth with different average grain sizes in the first layer (G_A) are presented. For each, the shape of the curve bears a strong resemblance to the experimental data shown in Fig. 2. From this similarity, it can be inferred that the process of growth on a polycrystalline substrate — by simple steps such as migration and bonding to the more stable sites — can spontaneously give rise to a grain size distribution of this form. Another feature of the results of the model is that the simulations with small substrate grains (low G_A) underwent a more rapid
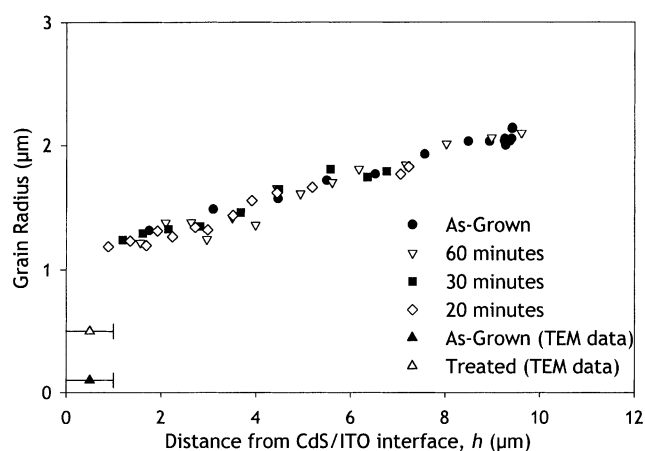

Fig. 2. Grain size development throughout the thickness of CdTe layers. The data in the main (apparently linear) series representing the bulk of the layer are from [9] and are invariant, even during severe processing with $CdCl_2$. The two points indicating very low grain size (TEM data) indicate that near-interface grain growth occurs beneath the otherwise stable CdTe grains during $CdCl_2$ treatment at 400°C for 20 min.
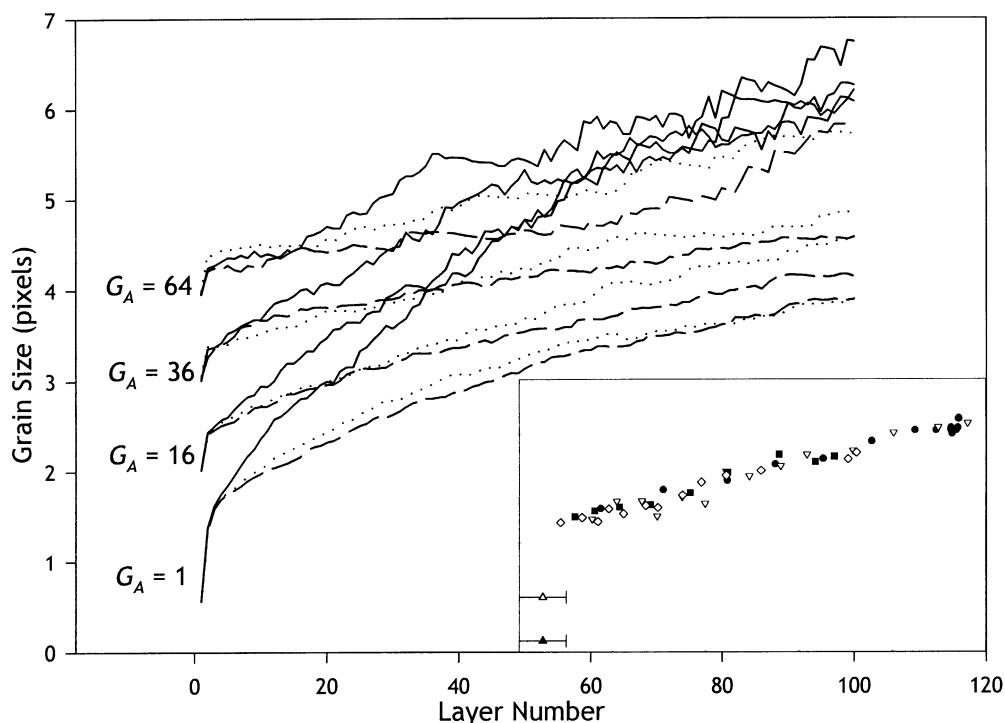
Fig. 3. Computer simulation of the development of grain size during growth on a polycrystalline substrate. The simulation takes place in a volume constructed from $100 \times 100 \times 100$ cubic cells. G_A is the average grain size in the first layer (substrate). Three simulations corresponding to different surface mobility factors are shown for each grain size. The inset shows the form of the experimental data (Fig. 2).

increase in grain size with layer growth than did those with larger grain size. (Note that this is not grain growth per se, as observed in the TEM study in Fig. 1. This is the development of a stable grain size distribution during growth.) From fitting the form of simulations of 1000 layers, a relationship between grain radius R and the layer thickness h of the form $R = a + kh^{-b}$ was found, with b in the range 0.5–0.6.

This observation that the smaller grains encourage a more rapid increase in grain size development may be considered in terms of the events that constitute the broadening of a grain: such events take place at the grain boundaries themselves. Only those species arriving or attaching to the surface near to a grain boundary participate in increasing the grain size. Hence, samples with a high grain boundary length per unit area (i.e. small-grained samples) are most likely to exhibit rapid grain size development. From the standpoint of the simulation, the ultimate limit of small grain size is the case of grains in the substrate comprising single cells, i.e. $G_A = 1$. Isolated species attaching to such a surface do so epitaxially and belong to the grain that sits directly beneath them. However, species that subsequently attach to an adjacent site do not belong to a different grain — the bonding criterion causes them to become attached to the first grain. Hence, for mono-cell polycrystalline substrates, grain size development is extremely rapid,

with increases of *at least* 100% occurring in the first monolayer.

3.2. Impurities

SIMS of the finished test structures, in the 'fresh' state and after 'light soaking' and 'bake testing' are shown in Fig. 4a–c, respectively. General features are that the $x = 0$ position on the graphs corresponds to the free surface of the Sb–Te contact layer, with the CdS layer being buried at a depth of 1.8–2.6 μm, the exact depth depending on the sample thickness. There is a prominent peak representing the CdS layer. The plateau of the oxygen signal represents the TCO layer; sputtering of the glass was not attempted. An important feature is the apparent peak in the concentrations of impurities in the vicinity of the CdS/TCO and this shall be discussed later. Quantitative profiles for S, Cl, Cu, Na, Sb and O are now discussed in turn.

Sulfur presents as a broad peak having a full width at half-maximum (FWHM) of 0.2 μm — even though the original layer was only 0.1 μm thick. This breadth is likely to be a convolution of instrumental effects (roughening of the SIMS crater) and genuine diffusion. The sulfur peak has a long tail, with sulfur being present in the CdTe at a level of 10^{20} cm^{-3} up to 2 μm from the CdS peak position. This is influenced relatively little
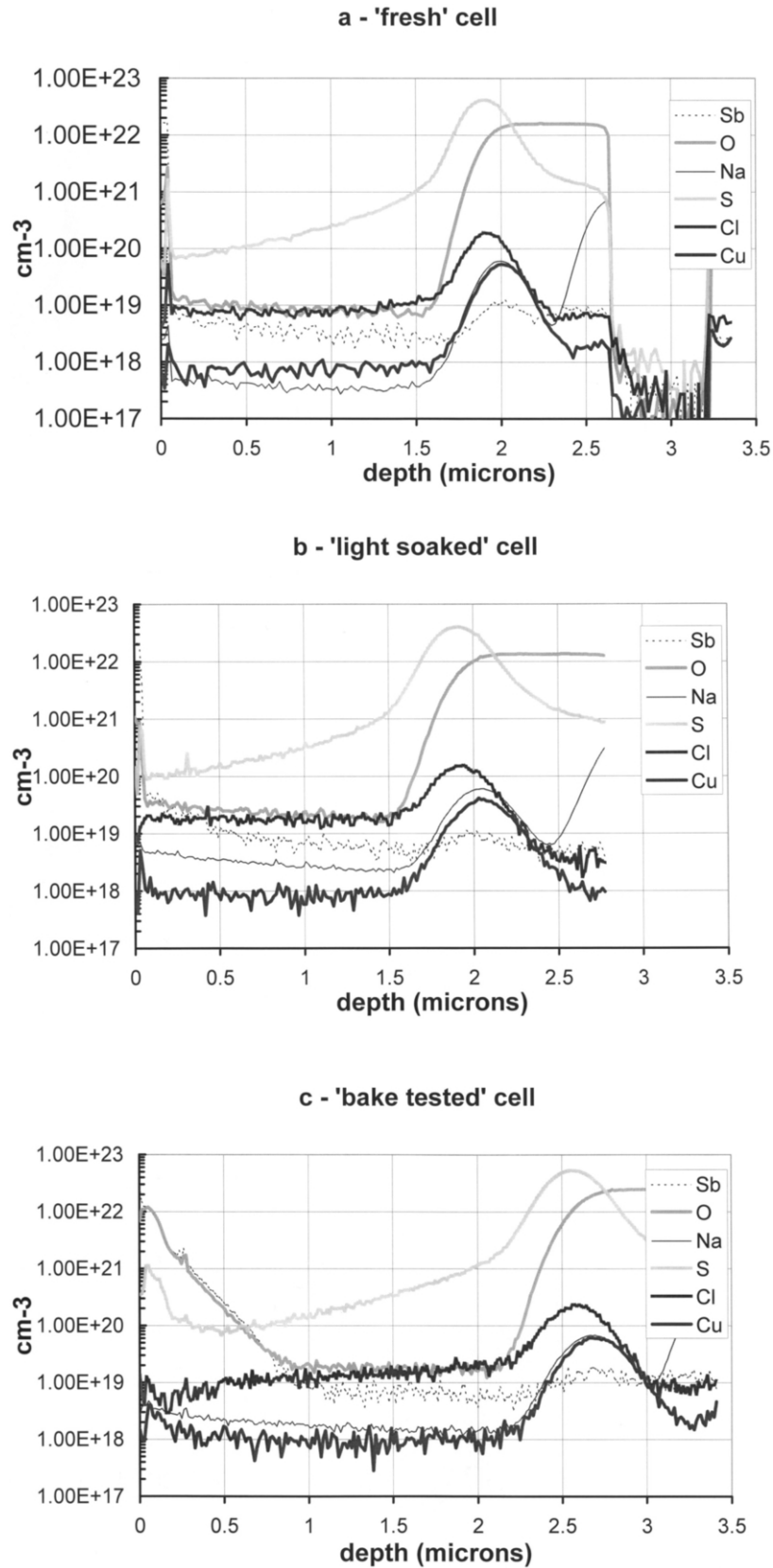
Fig. 4. Quantitative SIMS profiles for test structures comprising Sb–Te/CdTe(CdCl$_2$-processed)/CdS/TCO/glass: (a) 'fresh' device; (b) device subjected to 'light soaking' at 85°C for 1 week; and (c) device subjected to 'bake testing' at 400°C for 30 min.

by light soaking and by bake testing at 400°C, their effects being to broaden the S peak and increase its concentration only slightly. This small change indicates that the growth temperature of 500°C created a sulfur distribution that was substantially stable to further processing at lower temperature.

Chlorine is introduced into the cell material by processing and is present at a base level in the CdTe at 10^{19} cm^{-3}. The peak in Cl concentration corresponds very closely with the S peak in all cases. Light soaking and bake testing broaden the peak slightly and increase the apparent concentration by a maximum of five-fold. The increased concentration of Cl in the CdS position has been remarked upon before, see for example [12]. It may be speculated that Cl is simply more soluble in CdS than in CdTe, but the authors have been unable to find evidence of this in phase diagrams for example (the published phase diagrams do not include data for compositions close to the pure compounds). An alternative explanation is that the concentration is governed purely by grain boundary segregation and that the peak in the CdS arises because it has smaller grains than the CdTe. By assuming square columnar grains and using grain sizes of 0.05 μm for the CdS and 2 μm for the CdTe, the ratio of grain boundary area per unit volume is $2/0.05 = 40$. In fact, the apparent enhancement in concentration is approximately 25-fold in fresh material, but although this appears to be a good estimate, it is not evidence enough to prove this mechanism. An electrostatic mechanism of segregation is discussed with relevance to Cu and Na below.

Even though no Cu was intentionally introduced into these cells, the base concentration in the CdTe is approximately 7×10^{17} cm^{-3}. Strikingly, this is higher than the range of values reported by Asher et al. [17] for cells with Cu-loaded back contact materials (2–7×10^{17} cm^{-3}). There could be differences in the accuracy of the SIMS calibration in the two experiments, so perhaps detailed consideration of the absolute levels present would be inappropriate. The important point is that the Cu level in the present material is high. These cells were prepared from 99.999% pure CdTe, this corresponding to 10 ppm or 2×10^{17} cm^{-3} of impurities *in total*. As the level of Cu recorded exceeds this value, Cu may be considered not to arise solely from the starting CdTe. Other sources include the other layers in the cell, and also the processing environment and chemicals. Light soaking and bake testing do not appear to significantly influence the Cu concentration in the CdTe layer.

Sodium is expected to originate from the glass substrate. The base level of 3×10^{17} cm^{-3} in the CdTe increases by a factor of 10 upon light soaking or bake testing, and this acts to broaden the peak in the CdS too. The Na concentration peak always coincides with that of the Cu.

A recurring feature of these and other SIMS profiles [13] is that the peak in Cu and Na concentration is displaced from that of the S and Cl peaks. This displacement is always in the direction of the substrate. Although it would be helpful to have more accurate data, i.e. with enhanced depth resolution, three speculations about the origin of the displacement may be made. Firstly, the displacement between the peaks is ~ 0.1 μm, this being comparable to the thickness of the CdS. It may therefore be the case that the Cu peak is at the CdS/TCO interface, or even in the TCO itself. A second possibility is that the as-grown CdS layer contained a high proportion of Cu, and that during CdTe deposition and CdCl$_2$ treatment, the S profile diffused more quickly than the Cu profile. As Cu is considered to be a fast diffuser, the latter is unlikely unless the Cu is chemically bonded, perhaps as an oxide in the as-grown layer. (Whatever the explanation, this observation contradicts Dobson et al.'s suggestion that Cl and Cu are associated [12] — whilst not actually ruling out the complex centre that they suggest.) Thirdly, as both Cu$^+$ and Na$^+$ are monovalent positive ions, this suggests a mechanism for their displacement from the peak concentration of Cl$^-$ ions: The theory supposes that the separation of the negative and positive ions is in response to local band features at the SnO$_2$/CdS interface. Fritsche et al. [19] show that there can be upward band bending in the CdS at this interface — and that there is a conduction band plateau in the SnO$_2$. Hence, for electrostatic reasons, Cl$^-$ might be expected to accumulate in the potential well associated with the CdS. Similarly, Cu and Na might be expected to associate with the local upward band bending at the CdS/SnO$_2$ interface.

Sb is introduced from the top contact surface and room-temperature co-sputtering with Te appears to introduce a base level of 3×10^{18} cm^{-3} into the CdTe, this value not changing greatly upon baking, except near to the free surface. Baking at 400°C introduces significant diffusion over approximately 1 μm. This diffusion front is tracked by a corresponding oxygen concentration. Oxygen is present at approximately 2×10^{19} cm^{-3}, even in fresh cell structures.

SIMS has revealed vast concentrations of impurities in the CdTe, and further discussion of their origin, and of doping in these cells, is appropriate. Doping densities measured by *C–V* methods in the p-CdTe are generally in the range 10^{15}–10^{16} cm^{-3}. This is achieved by processing with CdCl$_2$, but as Dobson et al. point out [12], there is no consensus as to how cadmium chloride works to achieve doping. There is an apparent paradox that Cl, most often considered a donor, can be involved in p-doping. An audit of compensating impurities is perhaps instructive. The base CdTe is of 5 N purity, i.e. 99.999%, this representing 10 ppm or 2×10^{17} cm^{-3} impurities of unknown type. As the concentrations of impurities found in the cells by SIMS exceed this value

Table 1
A tentative audit of donors and acceptors in CdTe solar cells based on the present SIMS data-and an estimate of the V_{Cd} concentration that may be frozen in upon cooling from Te-saturated conditions during processing. Donors apparently outnumber the acceptors, but the material is actually p-type

Acceptors (cm^{-3})	Donors (cm^{-3})
V_{Cd}: 2×10^{16}	Cl: 8×10^{18}
Cu: 8×10^{17}	
Na: 3×10^{17}	
Sb: 3×10^{18}	

by one or two orders of magnitude, it is unlikely that the CdTe itself is their source. All other layers and processing steps must therefore be considered as sources of impurities if the SIMS is presumed to be accurate. Notwithstanding their origin, the concentrations of Cl, Cu, Na and Sb are at least approximately known for the purposes of audit. The concentration of native defects, most notably V_{Cd} (the cells are Te-rich), is not so easily quantified. The data determined by Greenberg [20] are most accurate for temperatures rather higher than the 400°C normally associated with processing. A tentative estimate of the cadmium vacancy concentration is 10^{16} cm^{-3}. The audit is shown in Table 1. From these rather incomplete data, it is evident that the density of acceptors is insufficient to compensate the density of Cl donors. Further discussion adds to the usual speculations as follows. Firstly, it is possible that there are as yet unidentified and unquantified acceptors; the role of O is not clear, for example, and it is not included in Table 1. Secondly, perhaps not all of the potentially electrically active species are actually active. Grain boundary segregation and dissolution in free Te may each contribute to absorbing the excess donors. A third possibility is that the concentration of cadmium vacancies vastly exceeds the estimate from equilibrium considerations. This would imply that some aspect of the CdCl$_2$ treatment, for example, introduces higher concentrations of V_{Cd} than can arise from heating alone. This latter suggestion is perhaps consistent with the work of Dhere [21], in which heat treatment alone was compared with heat treatment with CdCl$_2$ for CdTe grown at different temperatures. CdCl$_2$ always yielded better cells, but for CdTe grown at the higher temperatures, the effects of CdCl$_2$ and plain annealing began to converge. The implication remains that cadmium vacancies are important, but that chemical processes are perhaps responsible for their control.

4. Conclusions

For CSS-grown CdTe solar cells, the CdTe grain size distribution has previously been reported as being of the form $R = mh + c$, i.e. linearly increasing radius R with distance from the CdTe/CdS interface, h. Moreover, it was thought to be invariant with CdCl$_2$ processing. This study does not contradict those findings, but adds an understanding of the near-interface grain development, both during growth and processing. In processing, the near-interface grains undergo grain growth (from 0.1 to 0.5 μm) beneath an otherwise stable CdTe layer. However, the corresponding two-fold increase in J_{sc} is unlikely to result from this grain growth alone. Computer modelling of the development of grain size during growth confirms that the form of the grain size distribution experimentally observed can occur from additive processes. The form of the function of grain size R with distance from a polycrystalline interface is of the type $R = a + kh^b$ ($b = 0.5–0.6$) — and this approximates to $R = mh + c$ at large h.

Quantitative SIMS of S, Cl, Cu, Na, Sb and O were presented for Sb–Te contacted CSS cells that were either 'fresh', 'light soaked' at 85°C for 1 week, or 'bake tested' at 400°C for 30 min in air. Baking caused in-diffusion of Sb, together with oxidation to a depth of approximately 1 μm — and also raised the level of Na in the CdTe from 3×10^{17} to 3×10^{18} cm^{-3}. However, in general the levels of the impurities in fresh cells — and their distributions — were more striking than the changes caused by ageing or baking. The base levels of impurities in the CdTe approximately 2 μm from the CdS were: S, 7×10^{19}; Cl, 8×10^{18}; Cu, 7×10^{17}; Na, 3×10^{17}; Sb, 4×10^{18}; and O, 7×10^{18} cm^{-3}. Of these, Cl, Cu and Na increase in concentration by between one and two orders of magnitude in the vicinity of the CdS. Moreover, although the concentration peak for Cl correlates well with that for S, the maxima for Cu and Na are displaced towards the substrate by ~0.1 μm. Similar results are reported by other authors. However, from these measurements it is unclear whether these ions concentrate at, for example, the CdS/SnO$_2$ interface, or even in the SnO$_2$.

In considering the origin of the impurities measured, it is noted that their concentrations exceed the *total* impurity concentration expected in the 5 N (99.999%) grade CdTe used to grow the layers (10 ppm corresponds to 2×10^{17} cm^{-3}). Cl and Sb are introduced by deliberate processing. Na comes from the glass — at least in part. As no Cu was intentionally introduced, it is thought to come from either the growth and processing equipment, or else from the processing chemicals or other layers.

A simple audit of donor and acceptor species was performed and included a density of cadmium vacancies tentatively estimated from the Te-saturated phase diagram line at 400°C (~10^{16} cm^{-3}). This showed that the concentration of Cl species (~8×10^{18} cm^{-3}) vastly exceeds the density of acceptors considered in this survey. It is recognised that this preliminary survey is necessarily incomplete. However, it does highlight the

possibility that the concentration of V_{Cd} is greater than expected at equilibrium processing of pure CdTe at 400°C. Chemical contributions to the vacancy concentration, e.g. from $CdCl_2$ processing and self-compensation, cannot be excluded.

Acknowledgements

References

[1] R.W. Birkmire, E. Eser, Annu. Rev. Mater. Sci 27 (1997) 625–653.

[2] K. Durose, P.R. Edwards, D.P. Halliday, J. Cryst. Growth 197 (1999) 733–742.

[3] J. Werner, W. Jantsch, K. Frohner, H. Queisser, in: G.E. Pike, C.H. Seager, J. Leamy (Eds.), Grain Boundaries in Semiconductors, Elsevier, Amsterdam, 1982, p. 415.

[4] S. Pizzini, M. Acciarri, S. Binetti, S. Acerboni, Mater. Sci. Eng. B 24 (1994) 159–166.

[5] T.P. Thorpe, A.L. Fahrenbruch, R.H. Bube, J. Appl. Phys. 60 (10) (1986) 3622.

[6] L.M. Woods, D.H. Levi, V. Kaydanov, G.Y. Robinson, R.K. Ahrenkiel, 2nd World Conference and Exhibition on Photovoltaic Solar Energy Conversion, WIP, Vienna, 1998, p. 1043.

[7] S.A. Galloway, P.R. Edwards, K. Durose, Sol. Energy Mater. Sol. Cells 57 (1999) 61–74.

[8] H.R. Moutinho, R.G. Dhere, M.M. Al-Jassim, D.H. Levi, L.L. Kazmerski, J. Vac. Sci. Technol. A 17 (4) (1999) 1793.

[9] M.A. Cousins, K. Durose, Thin Solid Films 361/362 (2000) 253–257.

[10] Y.Y. Loginov, K. Durose, H.M. Al-Allak, S.A. Galloway, S. Oktik, A.W. Brikman, H. Richter, D. Bonnet, J. Cryst. Growth 161 (1996) 95.

[11] P. Capper (Ed.), Properties of Narrow-Gap Cadmium-based Compounds. B.L. Weiss (Ed.), EMIS Data Review Series, vol. 10, INSPEC, London, 1995.

[12] K.D. Dobson, I. Visoly-Fisher, G. Hodes, D. Cahen, Sol. Energy Mater. Sol. Cells 62 (2000) 295–325.

[13] D.S. Boyle, S. Hearne, D.R. Johnson, P. O'Brien, J. Mater. Chem. 9 (11) (1999) 6.

[14] H.C. Chou, A. Rohatgi, J Electron. Mater. 23 (1) (1994) 31.

[15] D.H. Levi, L.M. Woods, D.S. Albin, T.A. Gessert, D.W. Niles, A. Swartzlander, D.H. Rose, R.K. Ahrenkiel, P. Sheldon, 26th IEEE Photovoltaic Specialists Conference, Anaheim, CA, USA, IEEE, 1997, pp. 351–354.

[16] K. Durose, J.R.E. Sadler, A.J.W. Yates, A. Szczerbakow, 28th IEEE Photovoltaic Specialists Conference, Anchorage, Alaska, USA, IEEE, 2000, p. 487.

[17] S.E. Asher, F.S. Hasoon, T.A. Gessert, M.R. Young, P. Sheldon, J. Hiltner, J. Sites, 28th IEEE Photovoltaic Specialists Conference, Anchorage, Alaska, USA, IEEE, 2000, p. 249.

[18] K. Durose, D. Albin, R. Ribelin, R. Dhere, D. King, H. Moutinho, R. Matson, P. Dippo, J. Hiie, D.H. Levi, Inst. Phys. Conf. Proc. 164 (1999) 207.

[19] J. Fritsche, D. Kraft, A. Thissen, T. Mayer, A. Klein, and W. Jaegermann, Thin Solid Films, in press.

[20] J.H. Greenberg, J. Cryst. Growth 161 (1995) 1.

[21] R.G. Dhere, Study of the CdS/CdTe Interface and its Relevance to Solar Cell Properties, University of Colorado, Boulder, Co, USA, 1997, p. 160, PhD thesis.